Kinematic, lensing & X-ray mass estimates of a poor cluster

A. Biviano (Trieste, I)
+
P. Popesso, J.P.Dietrich, Y.-Y. Zhang,
G. Erfanianfar, M. Romaniello, B. Sartoris

Introduction

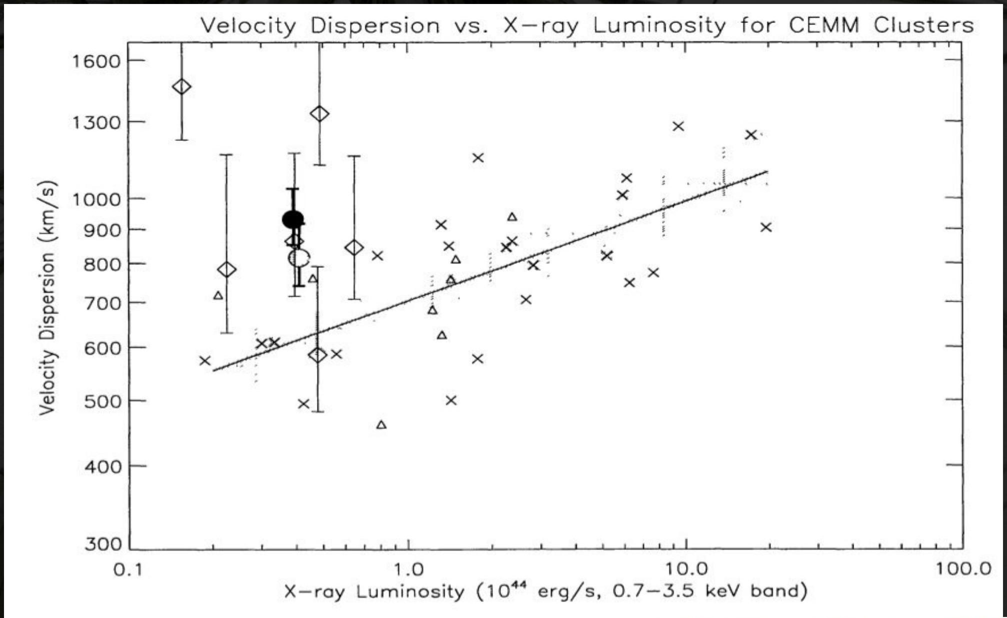

Bower+97: optically selected distant clusters have low L_X for their velocity dispersion, probably overestimated because of projection effects (filaments along the los) or because of a large population of infalling galaxies

Matching discrepancies X-ray and optical cluster samples *(Donahue+02, Gilbank+04, Basilakos+04, Sadibekova+14)*

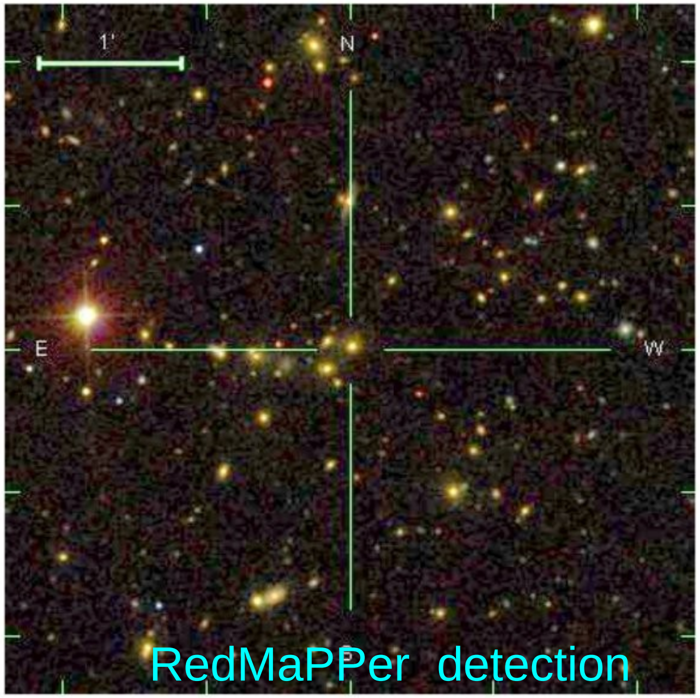

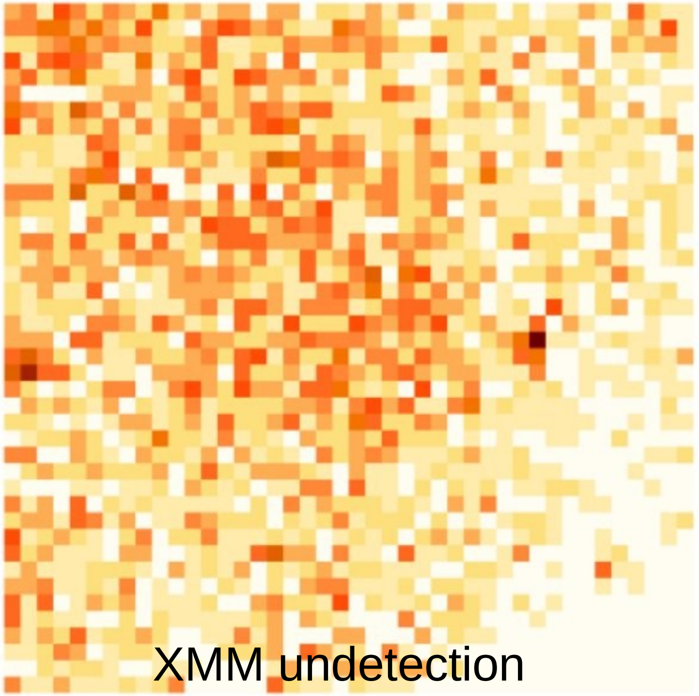

Introduction

Popesso, AB+07: “Abell X-ray Underluminous (AXU) clusters”:

spectroscopically confirmed Abell clusters with unsecure X-ray detection.

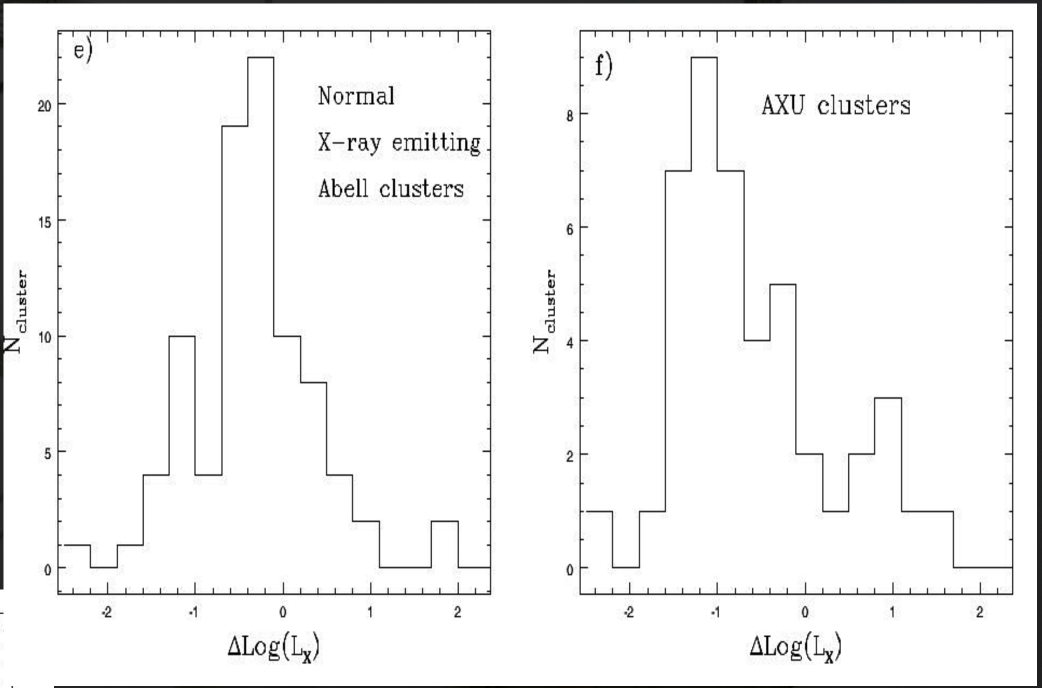

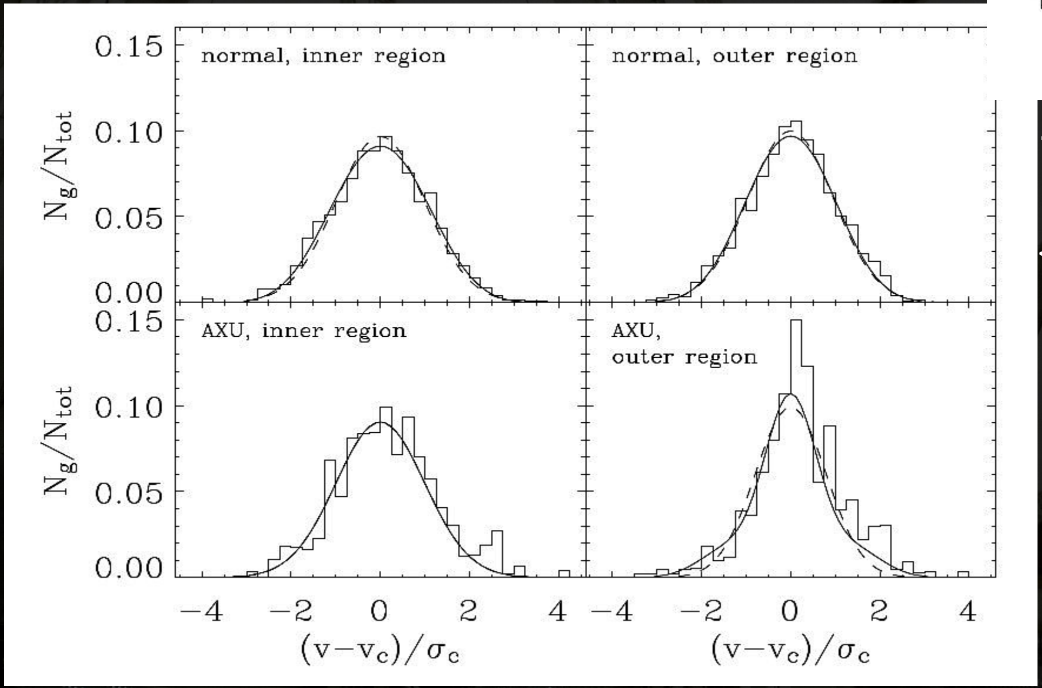

AXU stacked distribution of rest-frame cluster galaxy velocities is long-tailed in the outer regions, suggestive of an infalling population.

AXU clusters appear to have lower galaxy number density near the center than X-ray-normal Abell clusters, and higher bluer galaxy fraction.

Introduction

Dietrich, AB, Popesso+09: “Weak lensing observations of potentially X-ray underluminous galaxy clusters”: A315 @z=0.174 & A1456 @z=0.135, observed with WFI@ESO/MPG-2.2m to obtain their masses via Weak Lensing

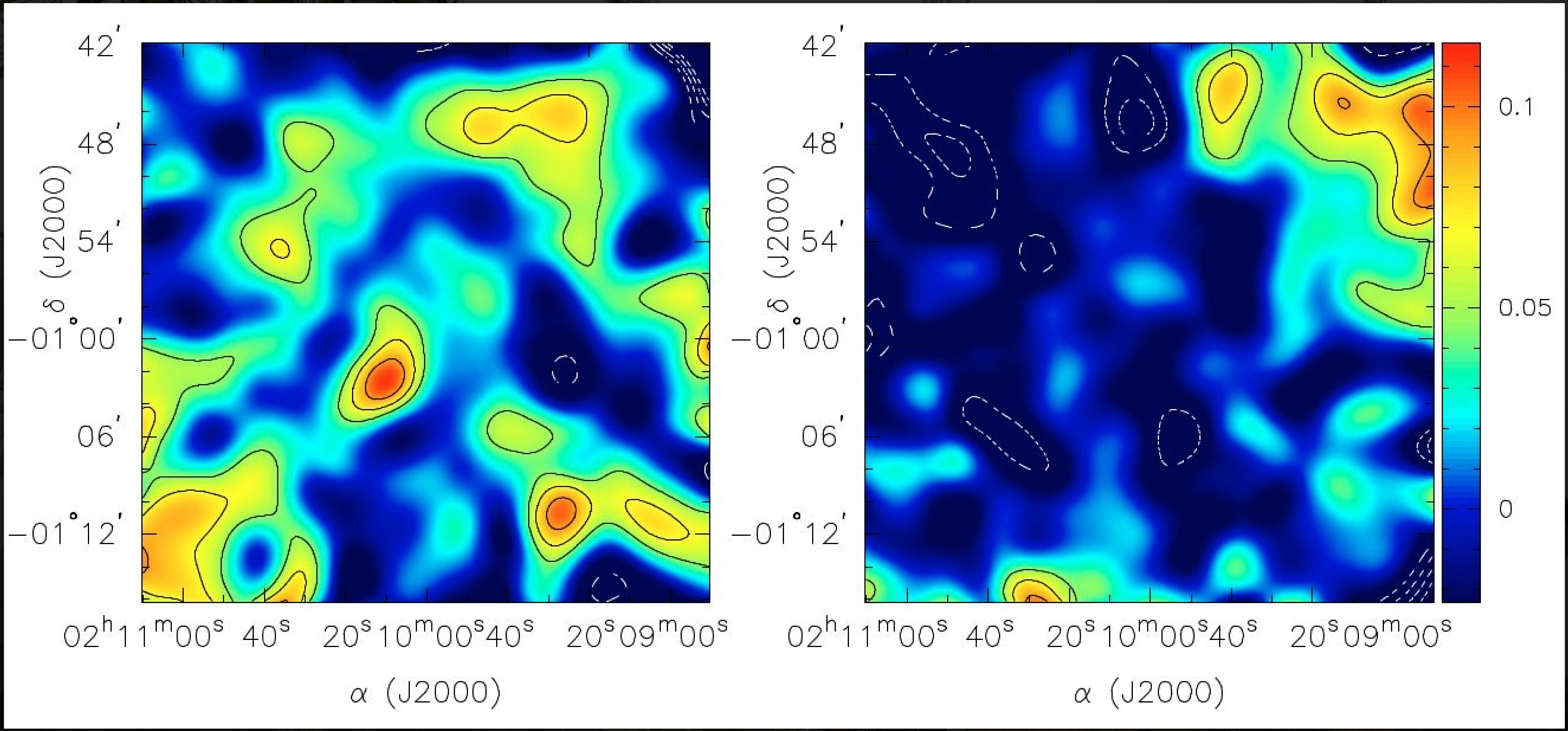

Weak Lensing Mass maps:
clear detection for A315 no detection for A1456

Introduction

Dietrich, AB, Popesso+09: “Weak lensing observations of potentially X-ray underluminous galaxy clusters”: A315 @z=0.174 & A1456 @z=0.135, observed with WFI@ESO/MPG-2.2m to obtain their masses via Weak Lensing

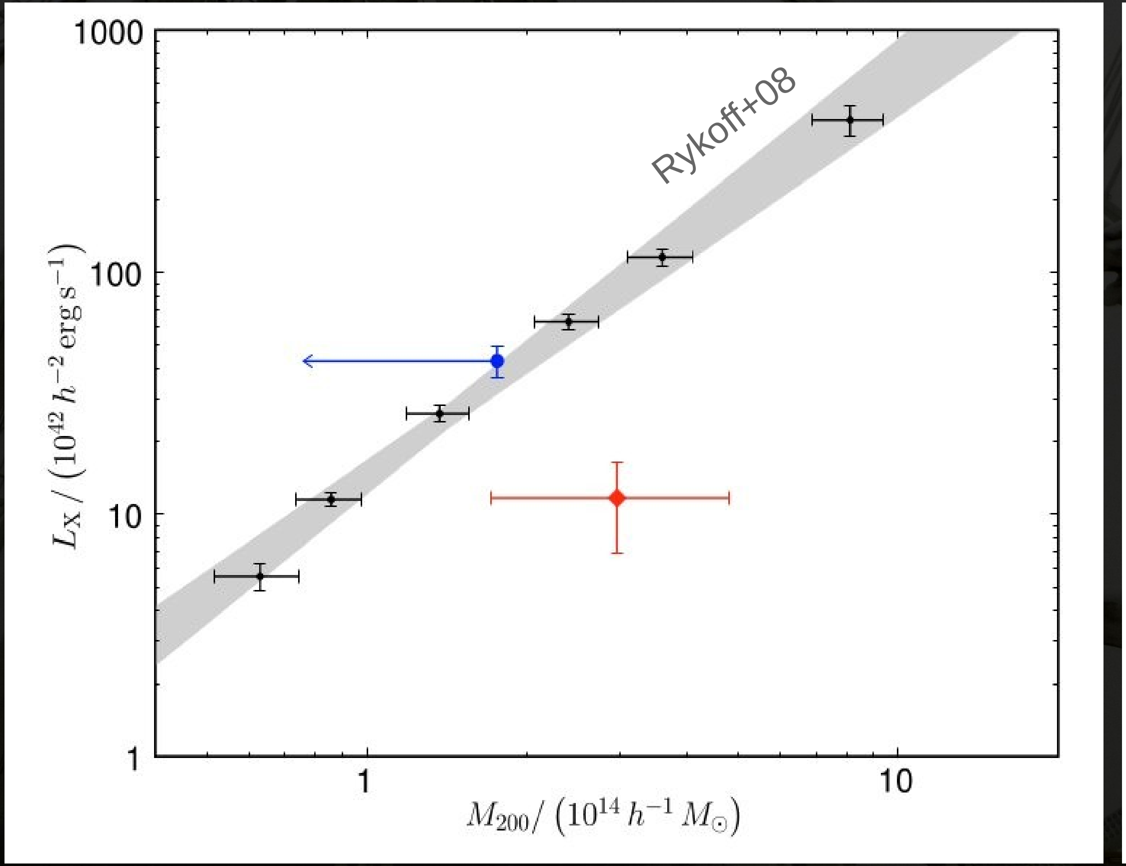

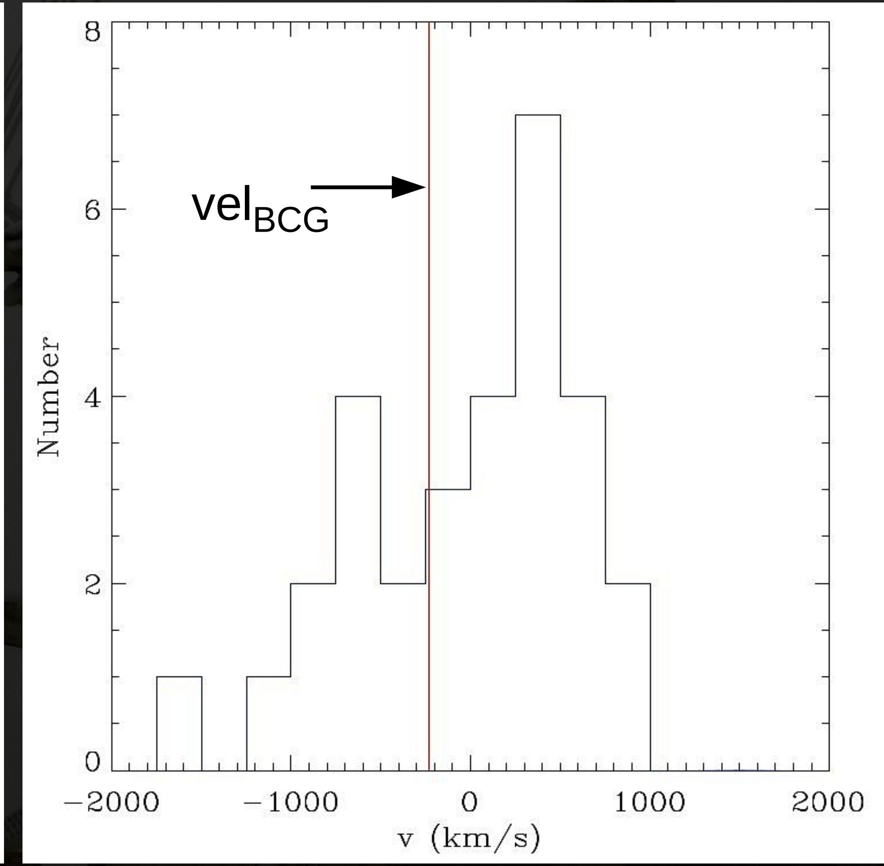

Masses from lensing confirms A315 is X-ray underluminous for its mass (AXU) while A1456 is not

Bimodal velocity distribution of A1456: unrelaxed dynamical state or projection effects → mass overestimate from velocity dispersion

A315: new data

VIMOS@VLT spectroscopic observations: 479 reliable redshifts, δv~110 km/s
+ SDSS-III DR10: 499 redshifts, 32 in common → total: 946 redshifts in 1° 12' x 45' field

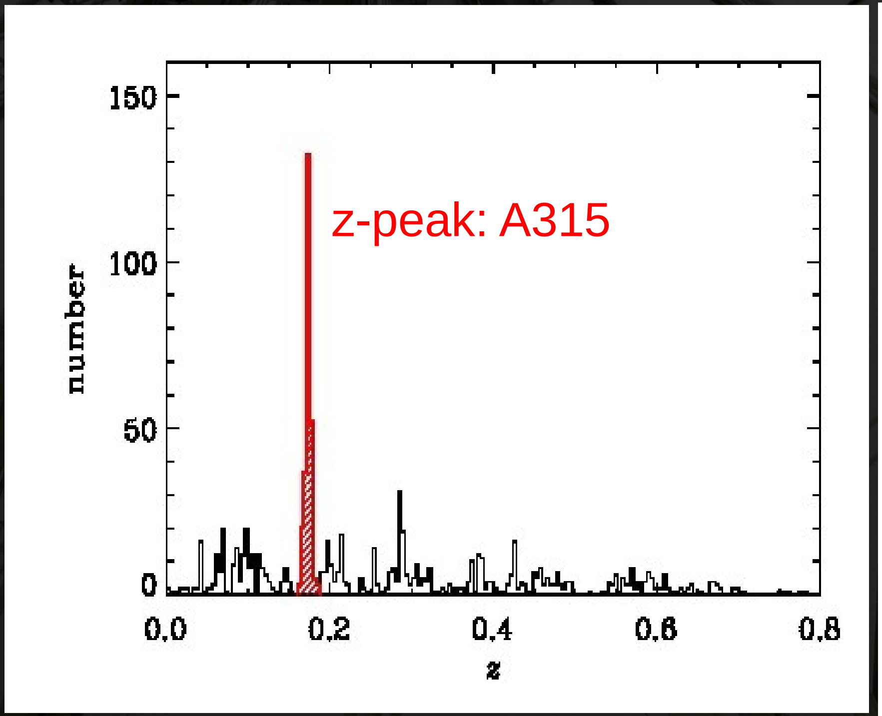

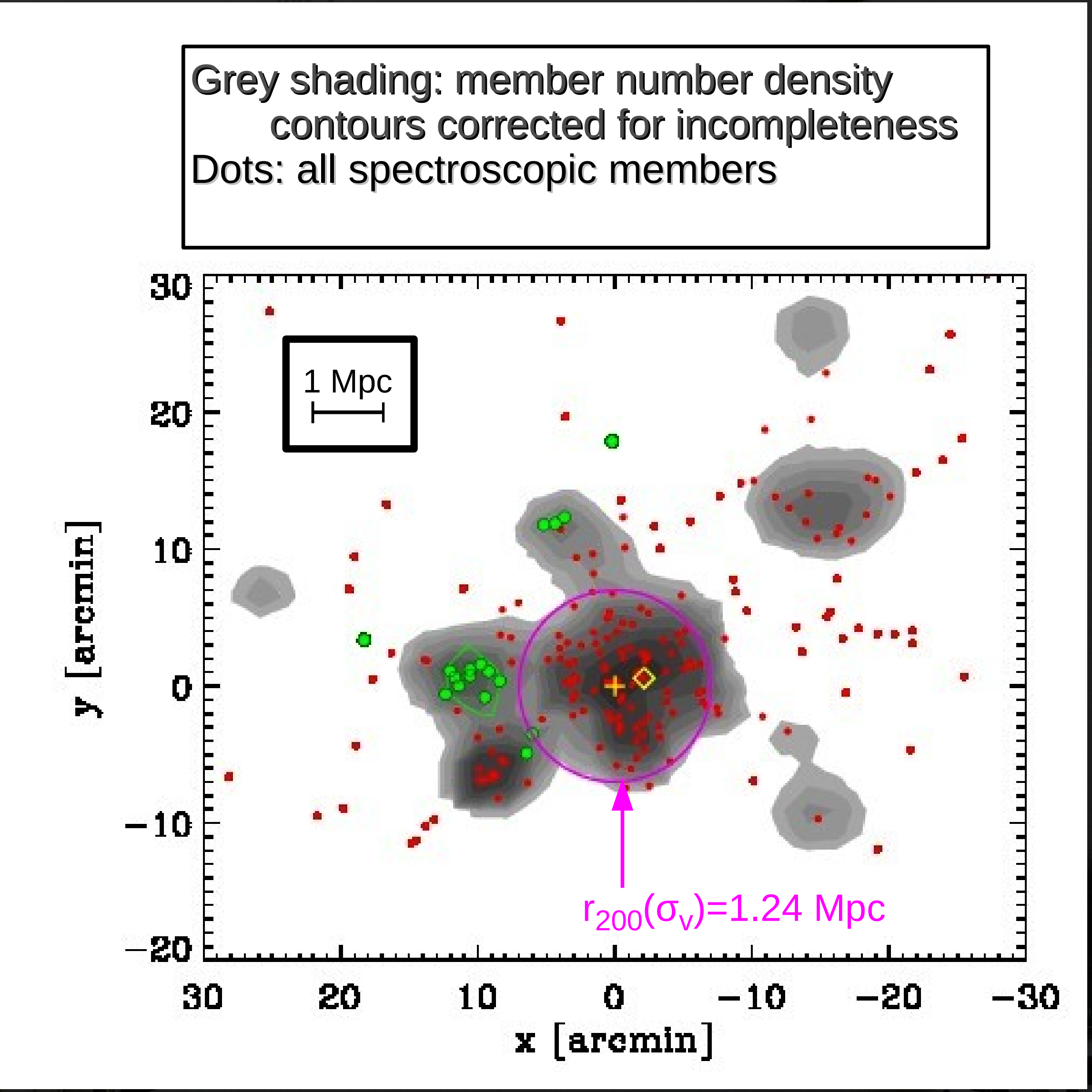

Number-density map of photometric members used to define cluster center as density peak (yellow +)
(yellow diamond: weak lensing peak from *Dietrich, AB+09*)

A315: members

Cluster members identified in projected phase-space diagram using the **Shifting Gapper** method (Fadda+96) – confirmed by the **Clean** method *(Mamon, AB, Boué 13)*

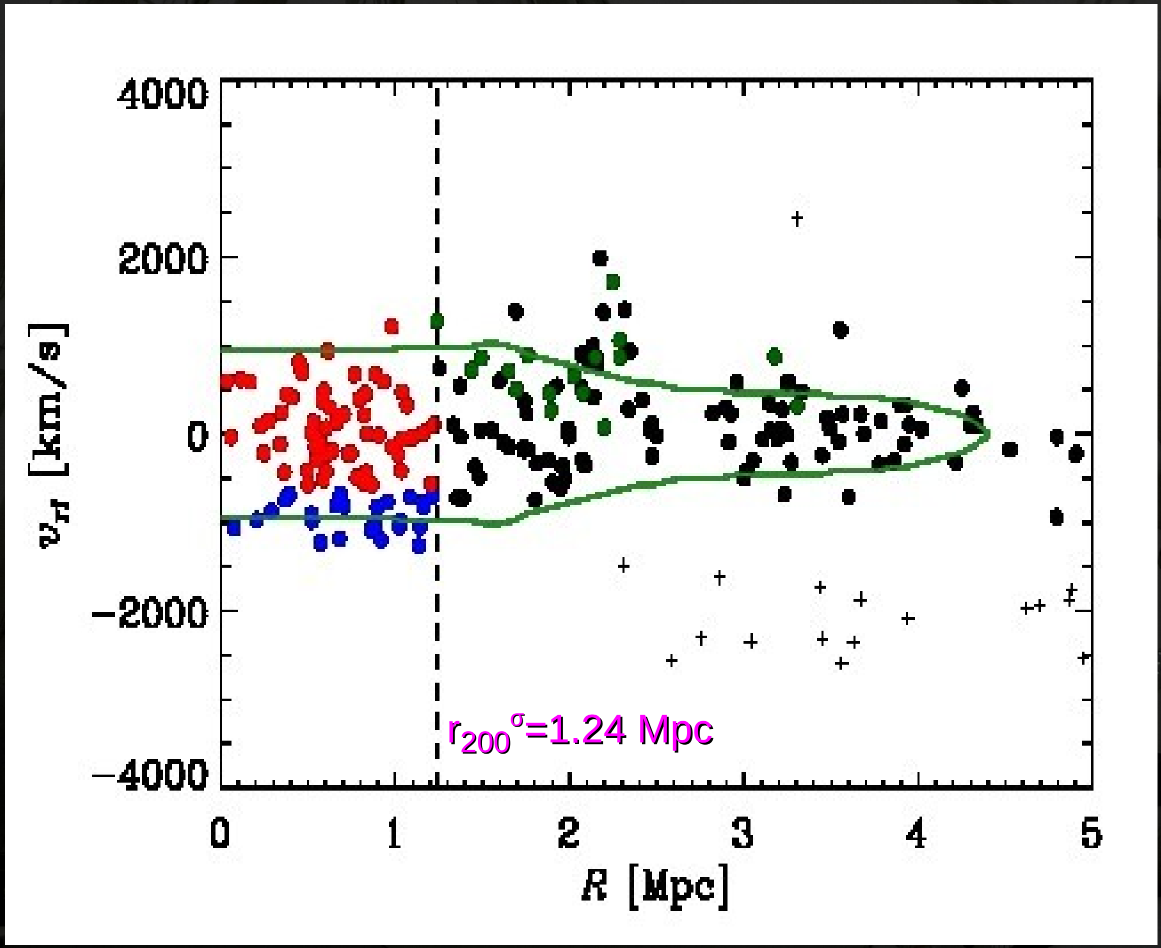

222 cluster members identified (filled dots)

σ_v= 603 ± 30 km/s

Assuming NFW M(r), mass concentration from c-M relation of Macciò+08, velocity anisotropy profile from Mamon+Łokas 05,

$\sigma_v \rightarrow\ r_{200}^{\sigma}$=1.24 ± 0.06 Mpc

Note: $G\ M_{200}=100\ H(z)^2\ r_{200}^3$

A315: substructures

Use the **DSb** algorithm *(AB+96,+02; after Dressler+Shectman 88)* to identify substructures:
17 cluster members assigned to subclusters (green dots) → 205 cluster members left

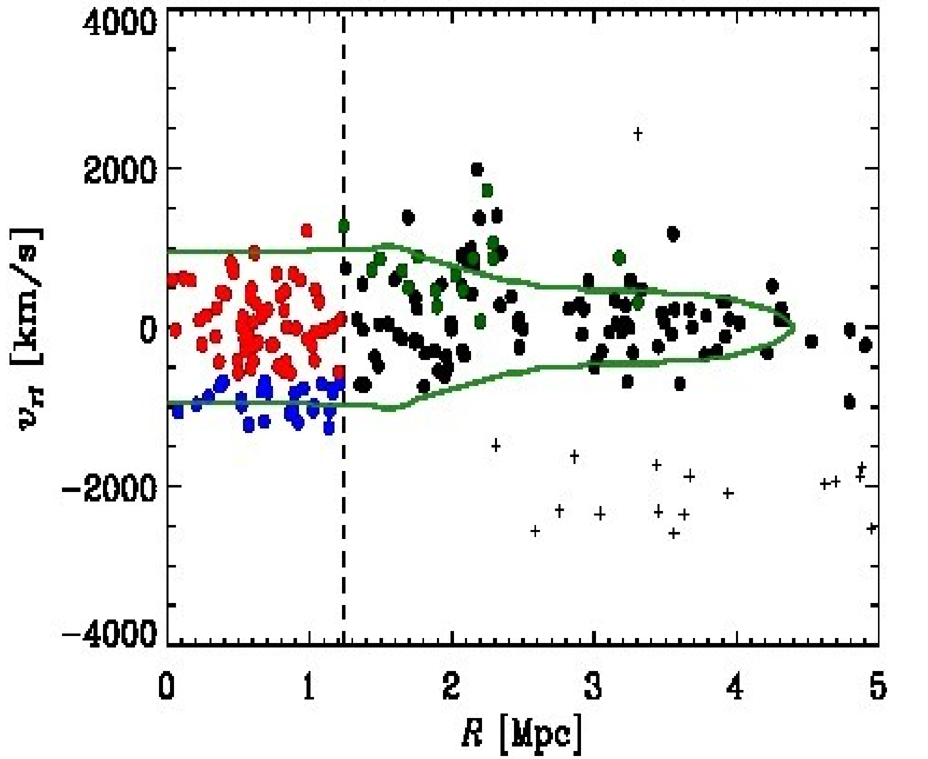

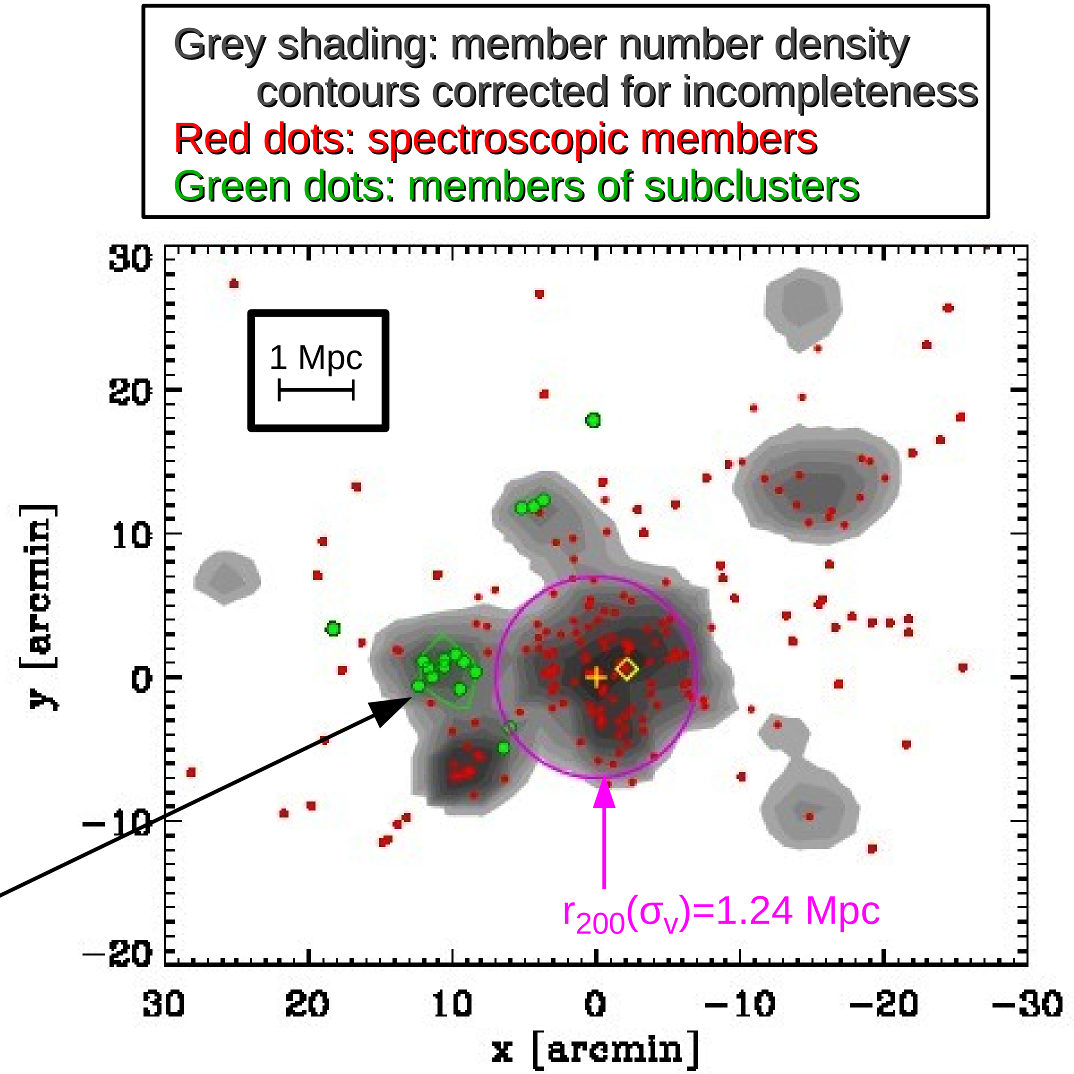

10 subcluster galaxies are in the same group, with σ_v= 282 ± 70 km/s

A315: substructures

Use **KMM** algorithm *(McLachlan & Basford 88; Ashman+94)* on remaining 205 members: chek for bimodality in velocity distribution.

2-Gaussian fit significantly better than 1-Gaussian fit for $R \leq r_{200}^{\sigma}$ velocity distribution.

1-Gaussian fit is adequate for $R > r_{200}^{\sigma}$ velocity distribution.

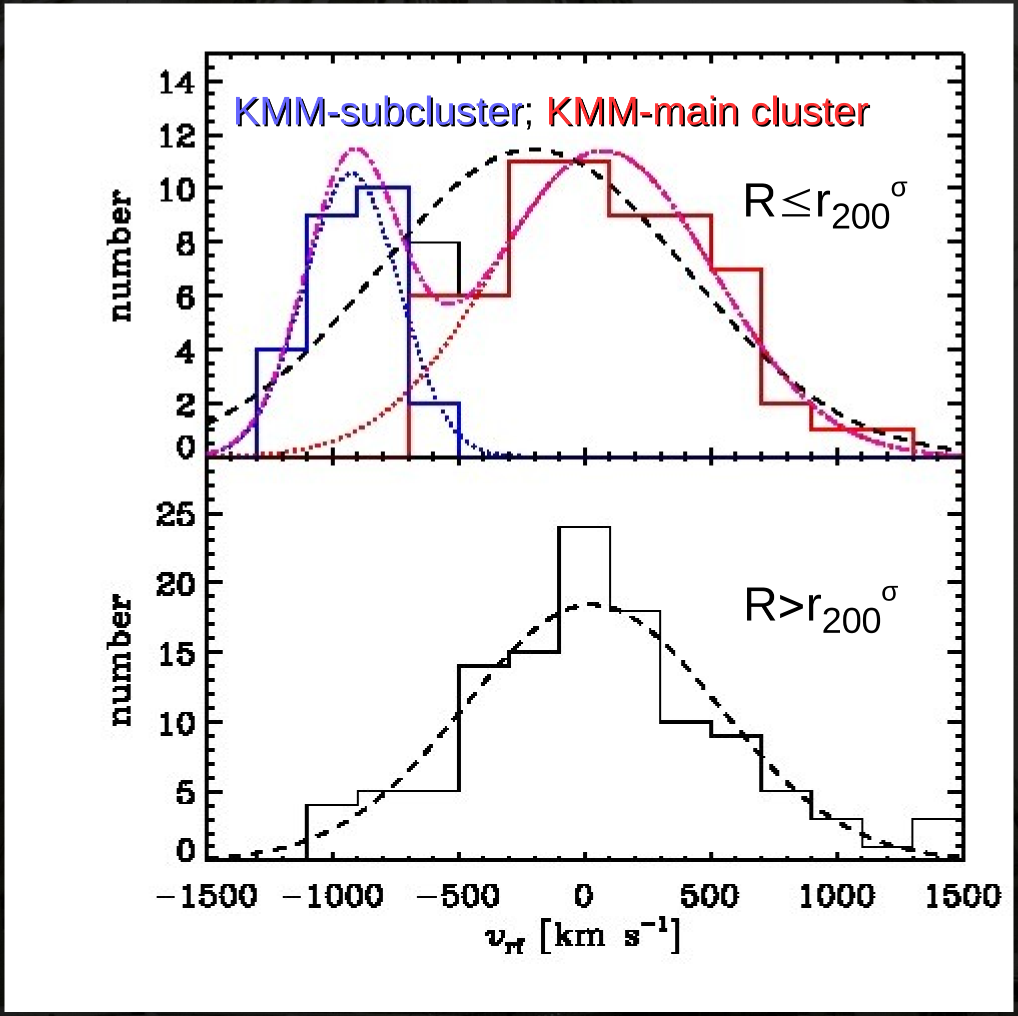

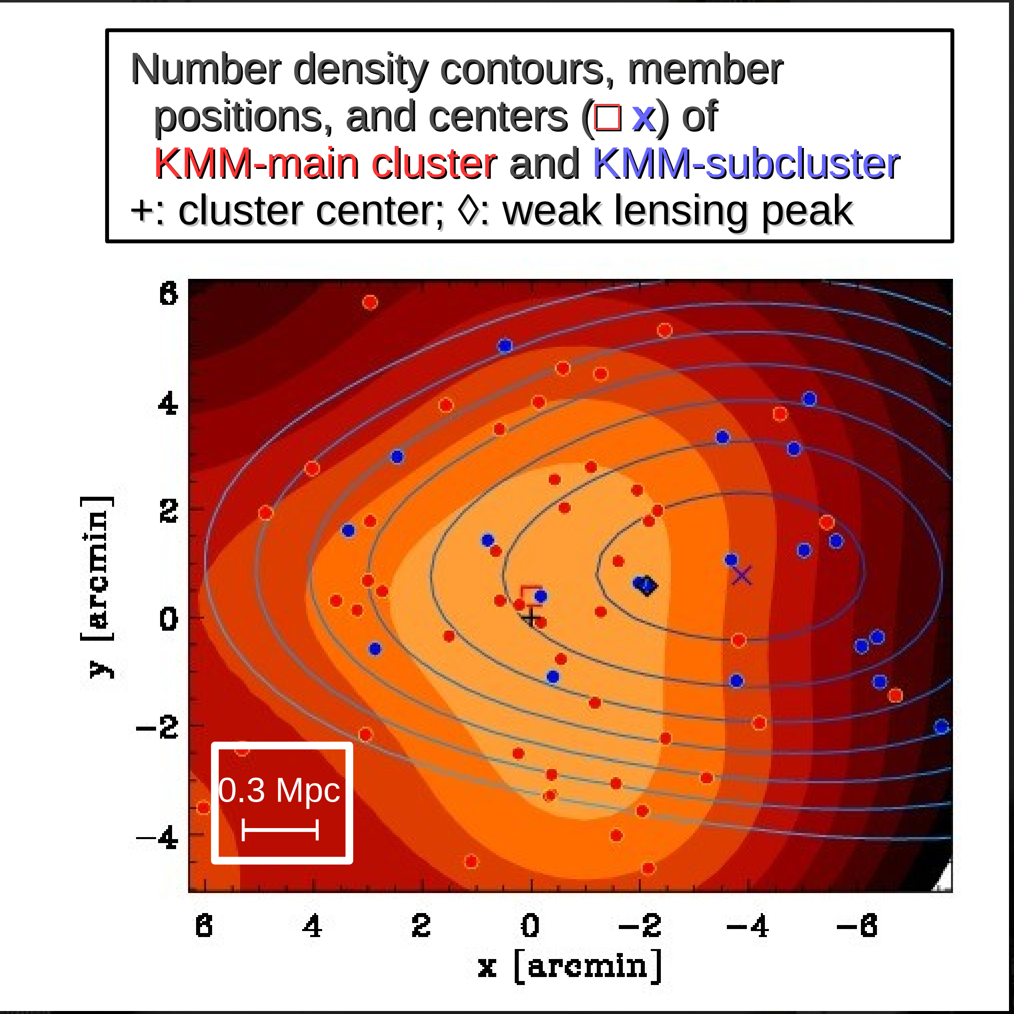

The centers of the inner KMM-main cluster and KMM-subcluster are 0.7 Mpc apart.

A315: mass profile

Caustic method *(Diaferio & Geller 97; Diaferio 99)*: discontinuity in projected-phase space is related to escape velocity of galaxies from the cluster potential. Method is robust vs. presence of subcluster → we do not remove DSb and KMM subclusters from the analysis

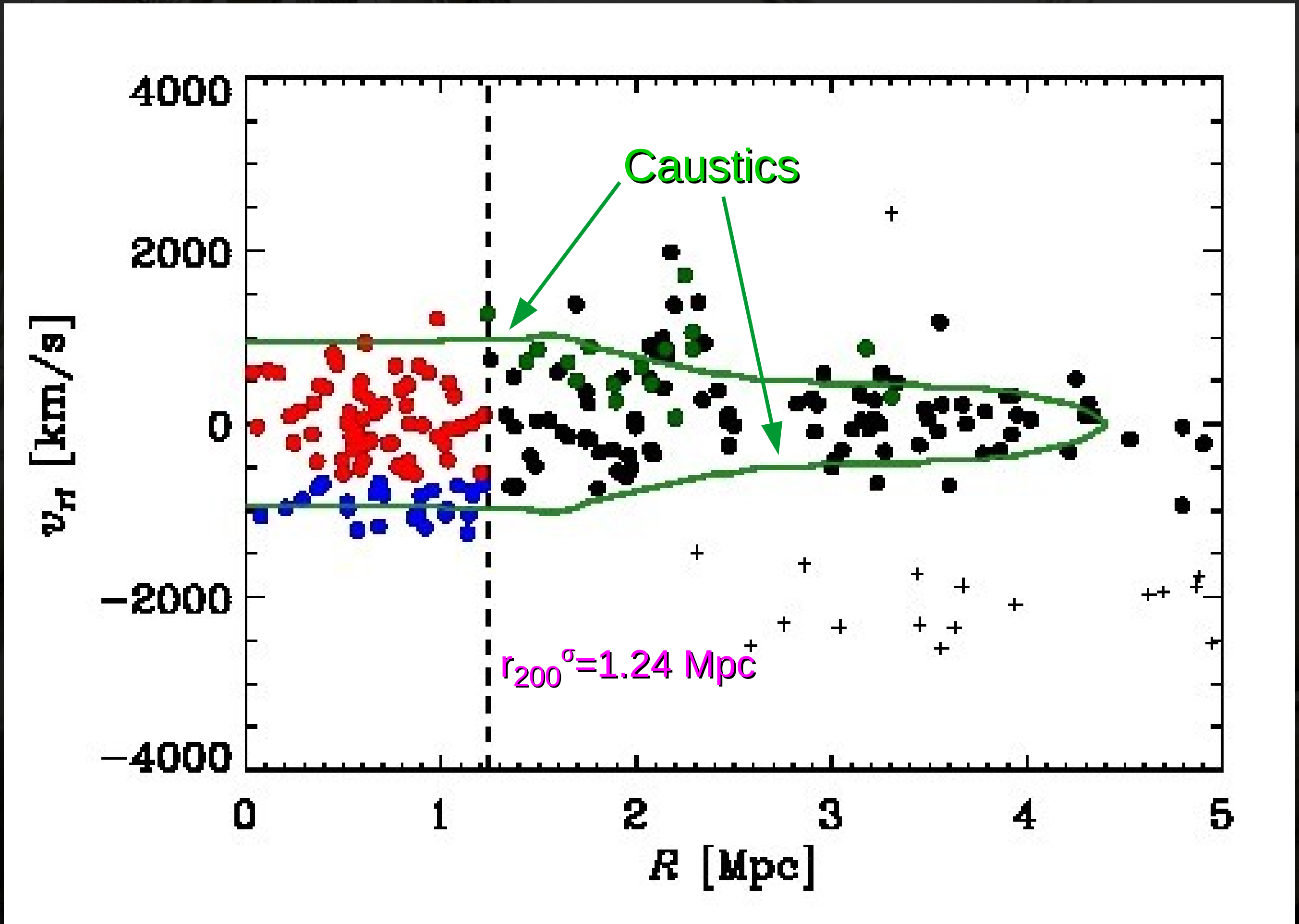

However this method does not provide strong constraints on the cluster mass:

r_{200}^{C}=0.9 [-0.3,+0.6] Mpc

At face value,
$r_{200}^{C} < r_{200}^{\sigma}$

A315: mass profile

MAMPOSSt method *(Mamon, AB, Boué 13)*: Maximum Likelihood analysis of the projected phase-space distribution of cluster members, finding best-fit for models of M(r) and the velocity anisotropy profile based on the Jeans equation for dynamical equilibrium.

Use $R \leq r_{200}^{\sigma}$ members, excluding DSb substructures; weigh the MAMPOSSt likelihood by the member probabilities of belonging to the KMM-main cluster

Red (**blue**) dots: cluster members with higher (resp. lower) probability of belonging to KMM-main

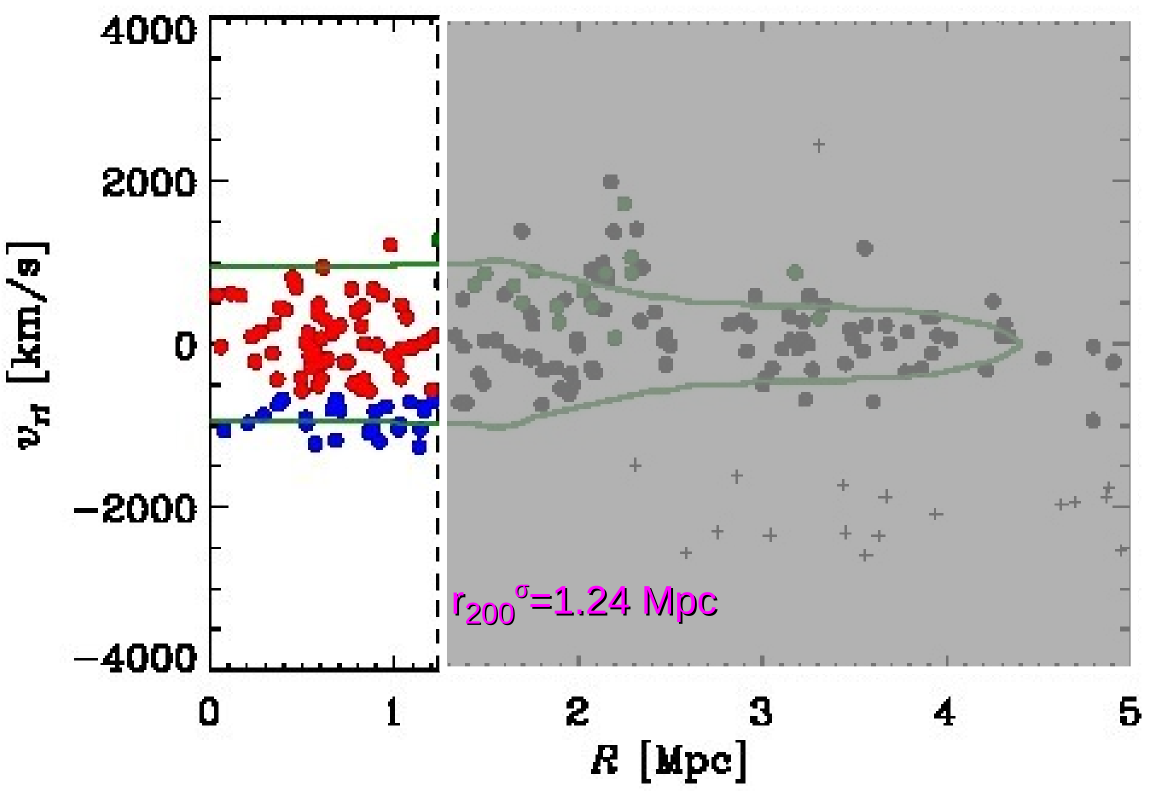

Use MAMPOSSt in 'Split' mode, fitting the spatial distribution of cluster members separately from their velocity distribution:

(projected) NFW with $r_{-2,\nu}$=1.0 [-0.3,+0.7] Mpc

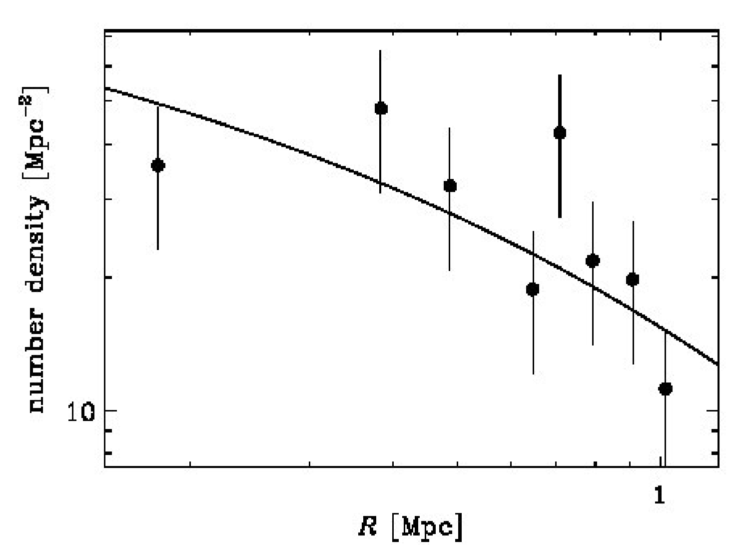

A315: mass profile

MAMPOSSt method *(Mamon, AB, Boué 13)*:

3 models for the mass profile M(r) - mass density profile ρ(r):

A) *Burkert 95*, ‘Bur’, $(d \log \rho / d \log r)_0 = 0$, $(d \log \rho / d \log r)_\infty = -3$
B) *Hernquist 90*, ‘Her’, $(d \log \rho / d \log r)_0 = -1$, $(d \log \rho / d \log r)_\infty = -4$
C) *Navarro+ 96,97*, ‘NFW’, $(d \log \rho / d \log r)_0 = -1$, $(d \log \rho / d \log r)_\infty = -3$

4 models for the velocity anisotropy profile $\beta(r) \equiv 1-(\sigma_t/\sigma_r)^2$:

a) constant, b) *Mamon+Łokas 05*, c) *Osipkov 79 + Merritt 85*, d) modified-*Tiret+07*

3 Free parameters:

(1) r_{200}, the mass profile normalization
(2) r_{-2}, the scale-radius of the mass profile
(3) a velocity-anisotropy parameter

M_{200}
M(r) concentration, $c \equiv r_{200}/r_{-2}$

A315: mass profile

Parameter	**NFW+T models**	Mean of all models
r_{200} [Mpc]	$0.85^{+0.16}_{-0.18}$	0.79 ± 0.02
r_{-2} [Mpc]	$2.1^{+6.5}_{-1.0}$	1.6 ± 0.2
$(\sigma_r/\sigma_\theta)_\infty$	$0.7^{+0.7}_{-0.3}$	0.8 ± 0.1

- NFW is best-fit M(r) model
- Tiret is bets-fit β(r) model
- Uncertainties in best-fit model *(filled blue dot)*
  $\gg$ variance among different models *(other symbols)*
  ➡ statistical error dominates
- Low concentration, $c \equiv r_{200}/r_{-2} < 1$
- Isotropic (or tangential) orbits

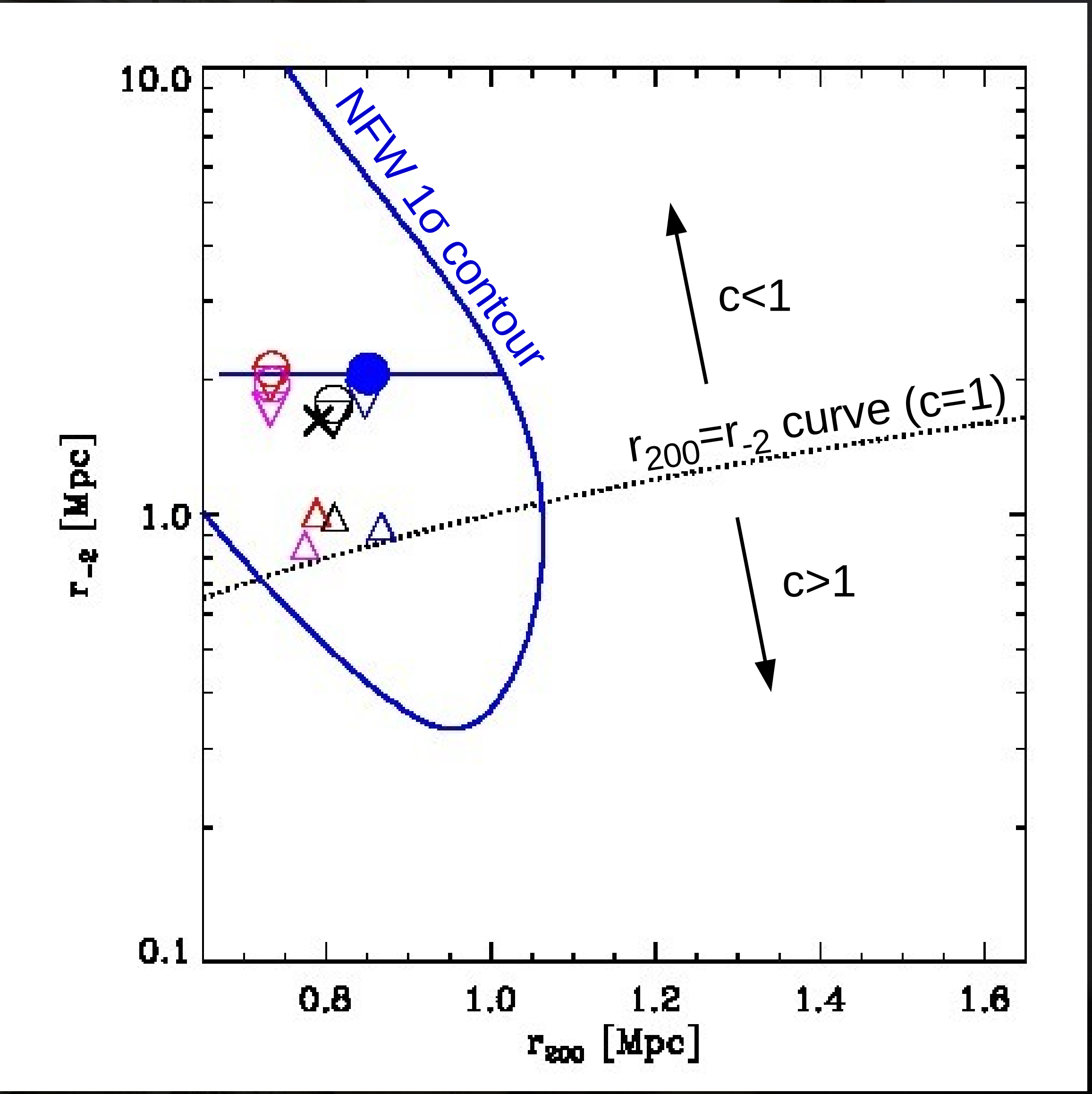

A315: mass profile

Parameter	NFW+T models	Mean of all models
r_{200} [Mpc]	$0.85^{+0.16}_{-0.18}$	0.79 ± 0.02
r_{-2} [Mpc]	$2.1^{+6.5}_{-1.0}$	1.6 ± 0.2
$(\sigma_r/\sigma_\theta)_\infty$	$0.7^{+0.7}_{-0.3}$	0.8 ± 0.1

- MAMPOSSt $r_{200} < r_{200}^{\sigma}$
- MAMPOSSt $r_{200} \approx r_{200}^{C}$
- Marginally inconsistent with the results from the kinematic analysis of *Dietrich, AB, Popesso+09* *(dashed line, shaded regions indicating random and random+systematic uncertainties)*

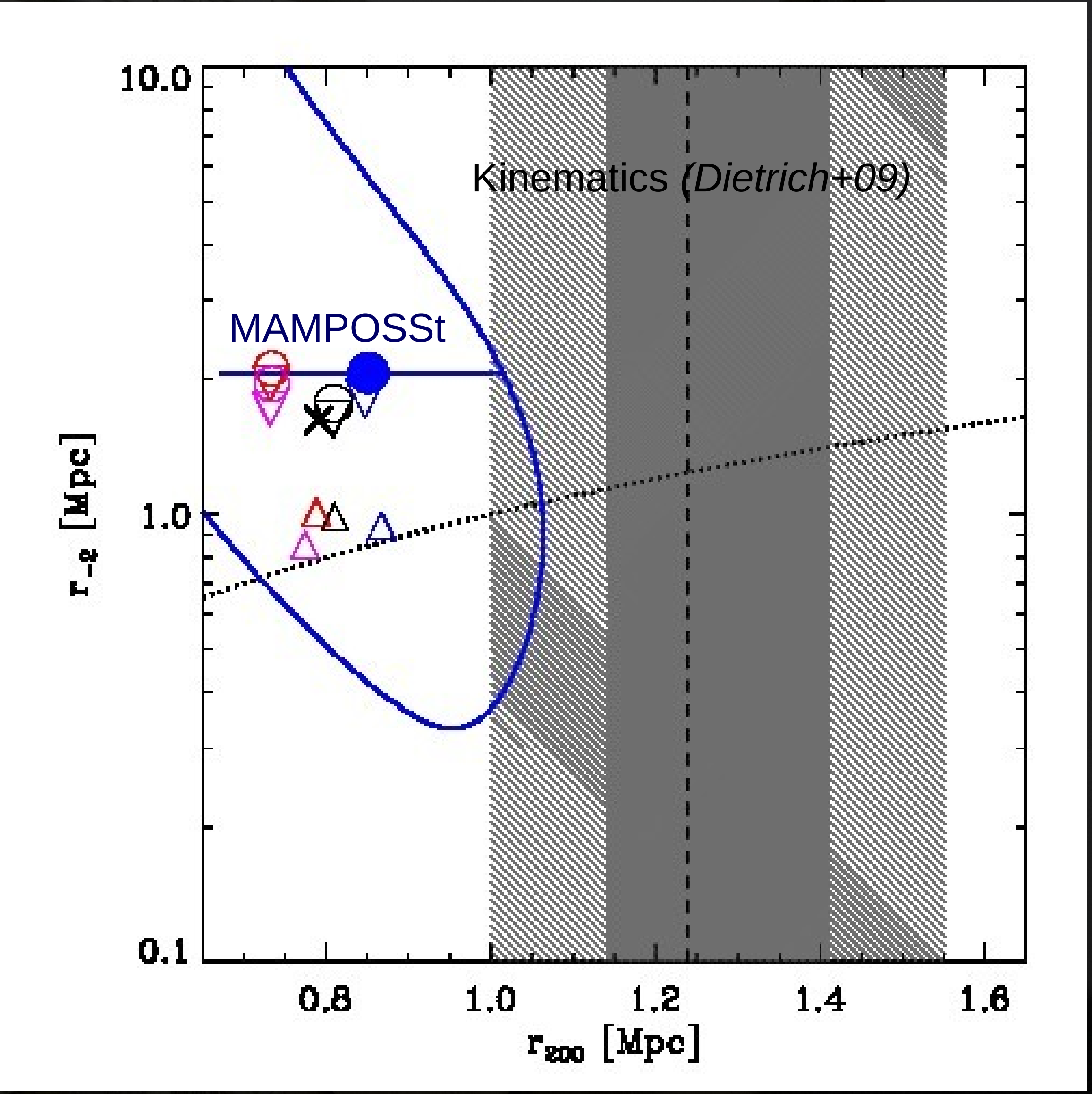

A315: mass profile

Parameter	NFW+T models	Mean of all models
r_{200} [Mpc]	$0.85^{+0.16}_{-0.18}$	0.79 ± 0.02
r_{-2} [Mpc]	$2.1^{+6.5}_{-1.0}$	1.6 ± 0.2
$(\sigma_r/\sigma_\theta)_\infty$	$0.7^{+0.7}_{-0.3}$	0.8 ± 0.1

- MAMPOSSt $r_{200} < r_{200}^{\sigma}$
- MAMPOSSt $r_{200} \approx r_{200}^{C}$
- Marginally inconsistent with the results from the kinematic analysis of *Dietrich, AB, Popesso+09* *(dashed line, shaded regions indicating random and random+systematic uncertainties)*

  ...and with the results from the weak lensing analysis of same authors *(red diamond with error bars)*

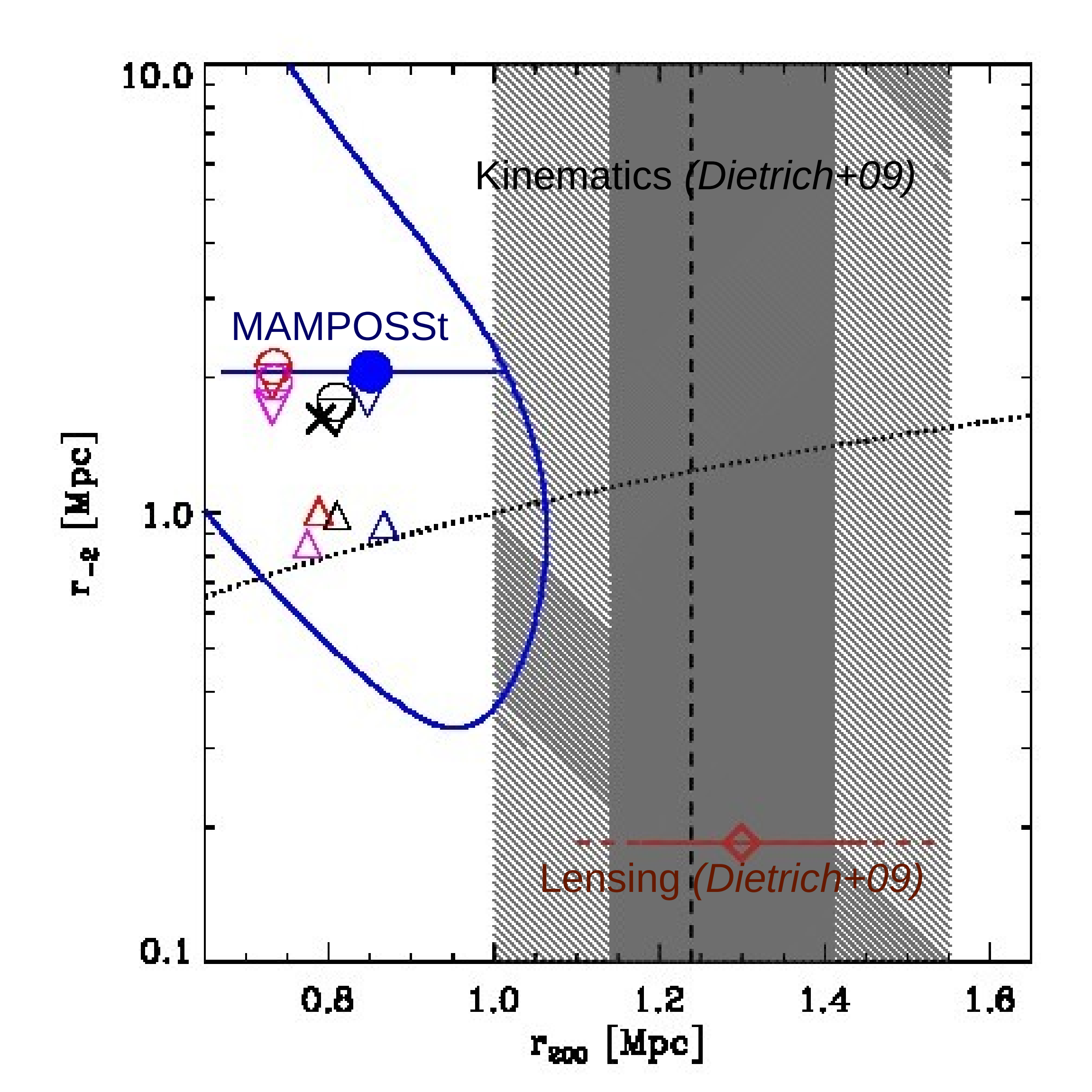

A315: mass profile

Parameter	**NFW+T models**	Mean of all models
r_{200} [Mpc]	$0.85^{+0.16}_{-0.18}$	0.79 ± 0.02
r_{-2} [Mpc]	$2.1^{+6.5}_{-1.0}$	1.6 ± 0.2
$(\sigma_r/\sigma_\theta)_\infty$	$0.7^{+0.7}_{-0.3}$	0.8 ± 0.1

- M(r) concentration
  $\ll$ theoretical expectation
  for given M,z (from *Correa+15*)

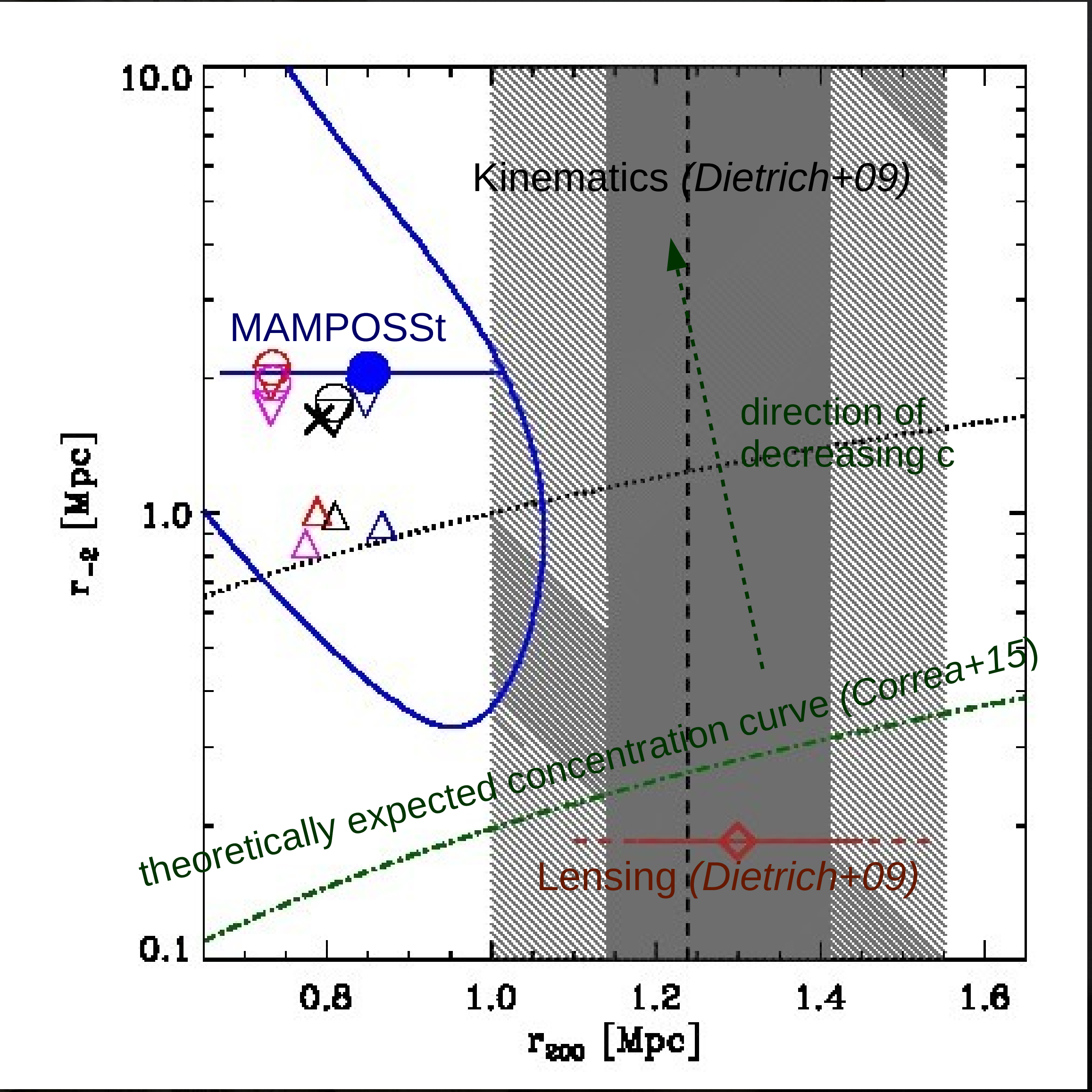

A315: mass profile

Parameter	NFW+T models	Mean of all models
r_{200} [Mpc]	$0.85^{+0.16}_{-0.18}$	0.79 ± 0.02
r_{-2} [Mpc]	$2.1^{+6.5}_{-1.0}$	1.6 ± 0.2
$(\sigma_r/\sigma_\theta)_\infty$	$0.7^{+0.7}_{-0.3}$	0.8 ± 0.1

Dietrich, AB, Popesso+09 derived r_{200}^{WL} from the weak lensing map, using NFW model fitting with fixed c=7 (theoretically motivated)

- Using c=1 we find: $r_{200}^{MAMPOSSt} \approx r_{200}^{WL}$ *(gold diamond)*

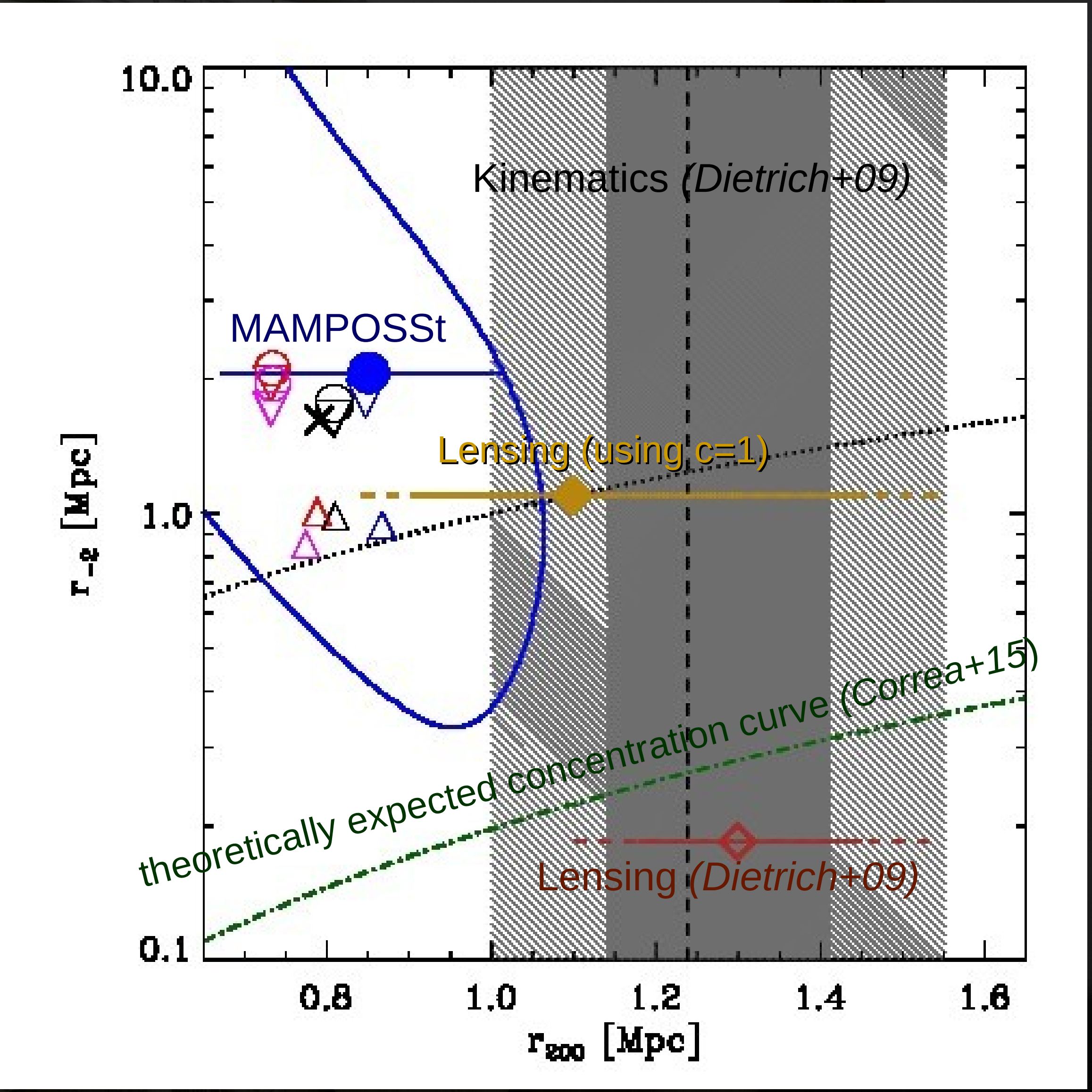

A315: mass profile

Method	M_{200} $[10^{14}\,M_{\odot}]$	Reference
Lensing	$3.0^{+1.2+0.7}_{-0.8-0.5}$	D09
Virial	$2.7^{+1.1}_{-0.7} \pm 1.0$	D09
L_X	$0.9^{+0.2}_{-0.2}$	D09
MAMPOSSt	$0.8^{+0.8}_{-0.7}$	This paper
Caustic $\mathcal{F}_\beta = 0.5$	$0.9^{+1.4}_{-0.9}$	This paper
Caustic $\mathcal{F}_\beta = 0.7$	$1.5^{+2.4}_{-1.4}$	This paper
Lensing with $c_{200} = 1$	$1.8^{+1.7}_{-0.9}$	This paper

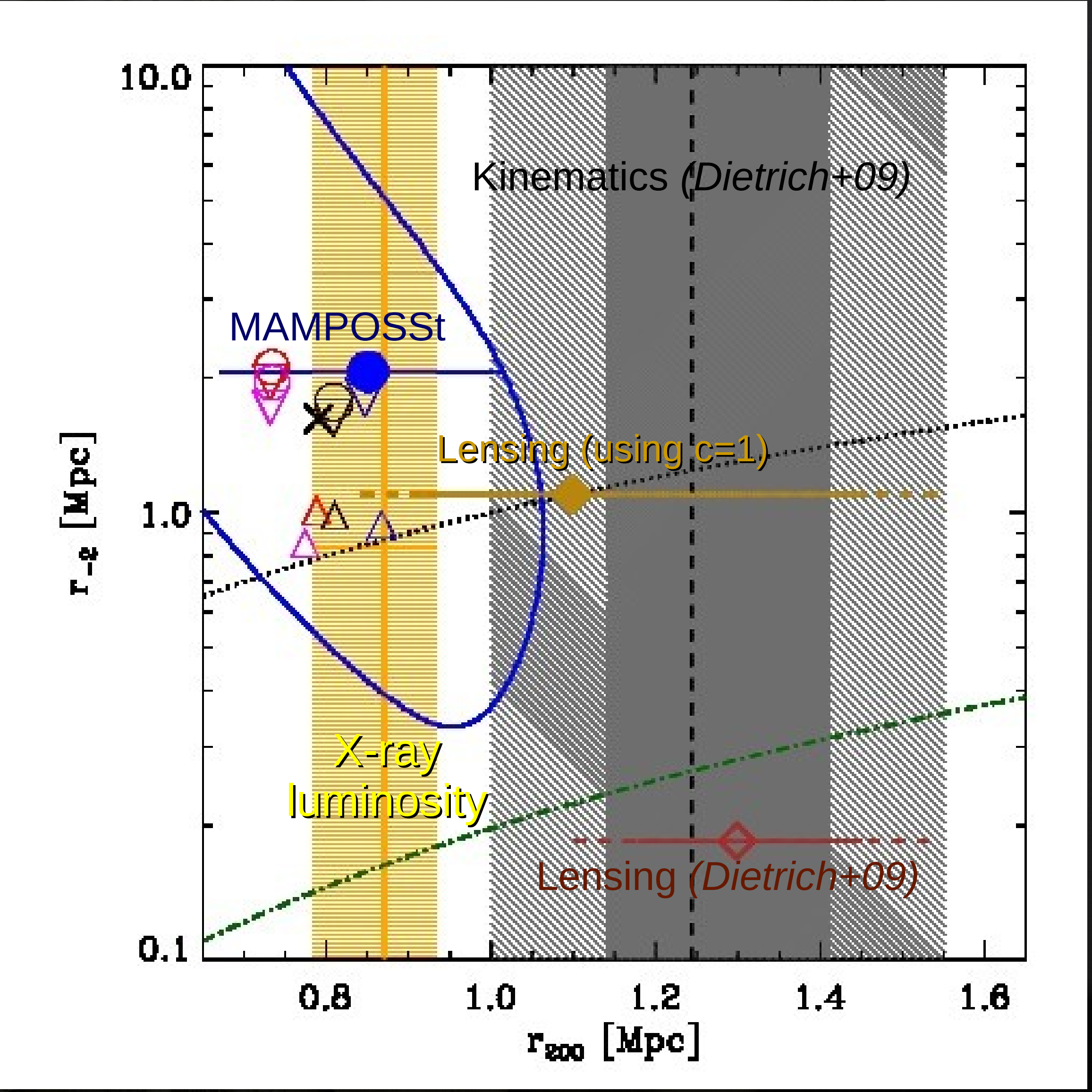

- The new r_{200} determinations (MAMPOSSt, lensing c=1) are in good agreement with r_{200}^{X} from L_X using the *Rykoff+08* scaling relation *(yellow line and shading)*

➞ A315 no longer X-ray underluminous

Conclusions

➔ A315 is a low-mass cluster (8×10^{13} $M_{\odot}$); this explains its low L_X

➔ Previous mass estimates were biased high because of:
  a) complex kinematics structure (unaccounted substructures)
  b) wrong assumption on M(r) concentration (lensing)

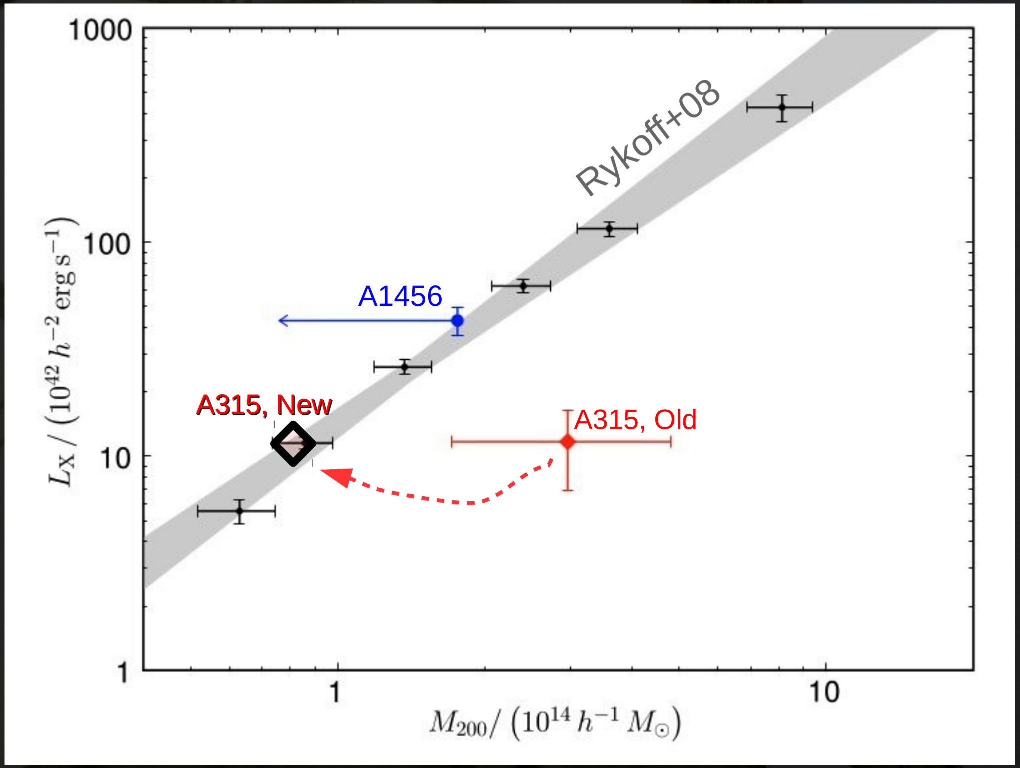

Conclusions

→ A315 is a low-mass cluster (8×10^{13} $M_\odot$); this explains its low L_X

→ Previous mass estimates were biased high because of:
   a) complex kinematics structure (unaccounted substructures)
   b) wrong assumption on M(r) concentration (lensing)

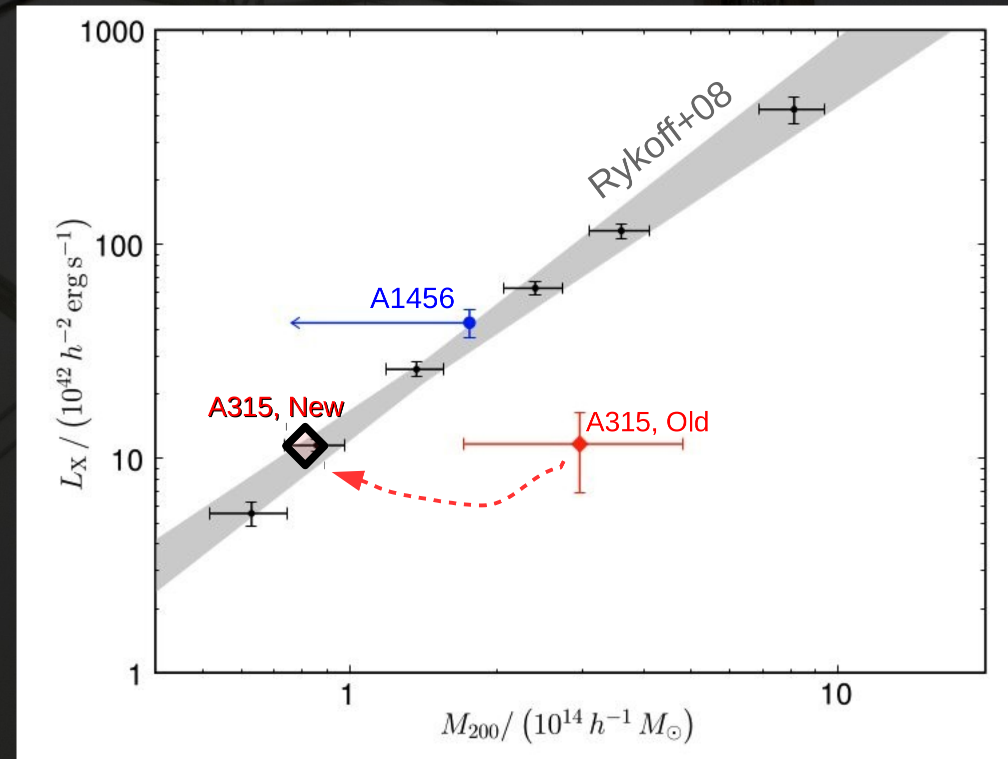

→ Can all Abell X-ray Underluminous clusters be explained by a wrong mass estimate caused by line-of-sight, infalling structures *(Bower+97)*?

Conclusions

➔ A315 is a low-mass cluster (8×10^{13} $M_\odot$); this explains its low L_X

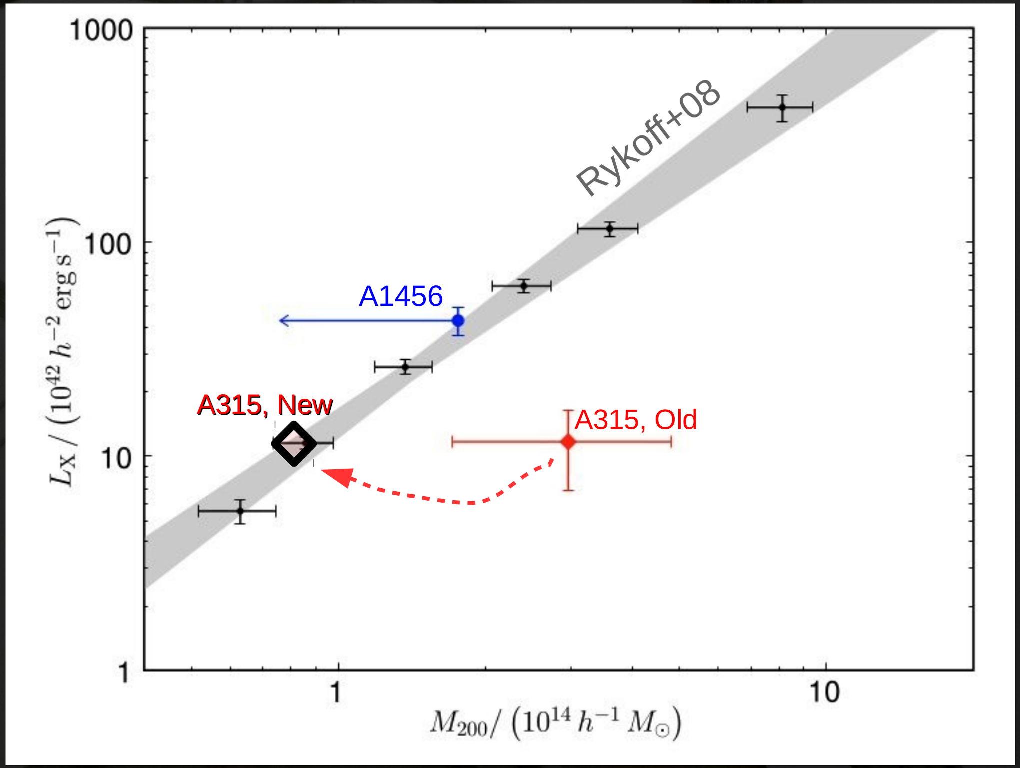

➔ Previous mass estimates were biased high because of:
   a) complex kinematics structure (unaccounted substructures)
   b) wrong assumption on M(r) concentration (lensing)

➔ Can all Abell X-ray Underluminous clusters be explained by a wrong mass estimate caused by line-of-sight, infalling structures *(Bower+97)*?

...the game is not quite over yet…

Conclusions

➔ Both A315 and A1456 appear to be in a (minor?) merging process (also: tangential orbits)

➔ The low-concentration measured for A315 is uncommon (both observationally, e.g. *Groener+16*, and theoretically, e.g. *Correa+15*); it could originate from the merging process; could this also lower L_X?

➔ *Planck collaboration 2016*: "*Planck* 2015 results. XXVII. The second *Planck* catalogue of Sunyaev-Zeldovich sources": some clusters have SZ Y_{500} compatible with their redMaPPer richness λ, but too high for their L_X
Are both λ and Y_{500} biased high, or are their X-ray underluminous for their mass?

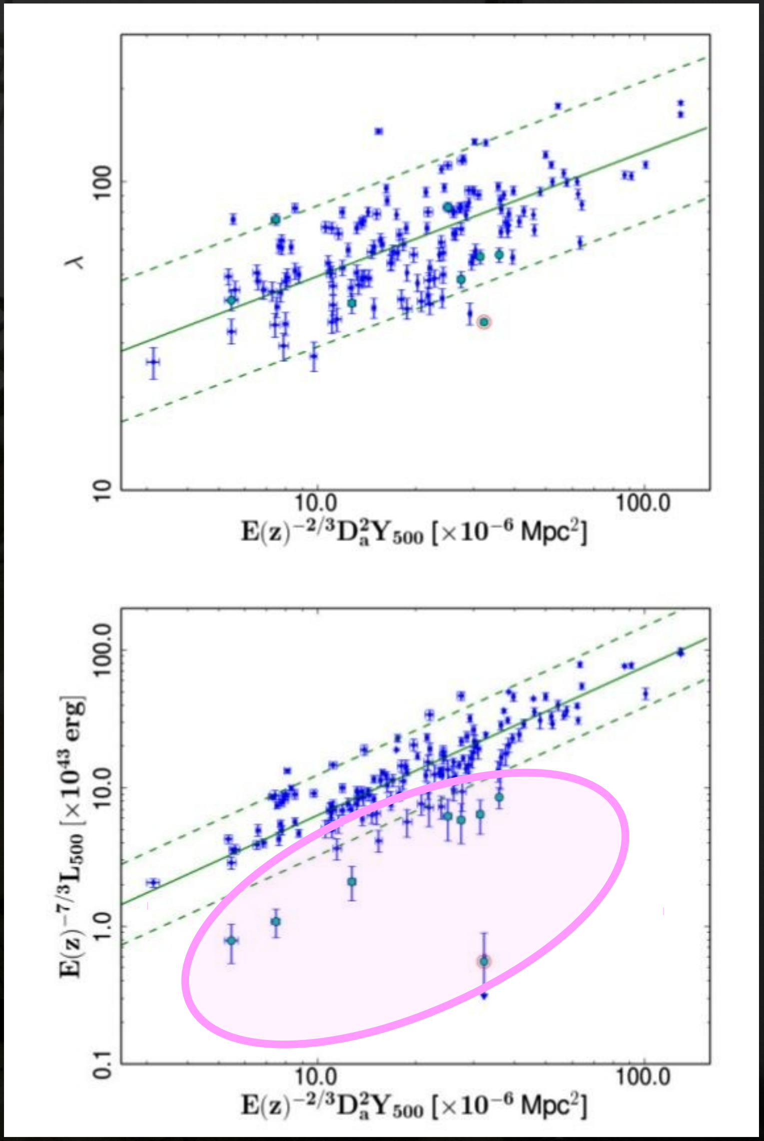

See also talk by Ewan O'Sullivan: some X-ray groups might remain undetected (mergers, non-CC, AGN-disrupted...)

Conclusions

Need follow-up observations of more candidate X-ray underluminous clusters for the issue to be settled down

Nice score if it was a soccer game, but looks like it's a basketball game!